Draft
May 22, 2002

Simulation of the interaction of 511 keV photons with a PET detector using GEANT4

M. Chamizo
Université de Genève

Abstract

The interaction of 511 keV photons hitting on a modulus of a PET detector is studied to determine the feasibility of reconstructing the energy and position of the photons and the probability to detect them. The material used to simulate a PET modulus is YAP:Ce. The analysis of the events whose first interaction is a photo-absorption and also the events that undergo first a Compton interaction and then a photo-absorption reveals that the coincidence detection probability is P $\simeq$ 0.46%.

Density ρ(g/cm^3)	5.55
Effective atomic charge Z	32
Scintillation light output (photons/MeV)	1800
Wavelength of max. emission (nm)	370
Refractive index n at 370 nm	1.94
Bulk light absorption length L_a (cm) at 370 nm	14
Principal decay time (ns)	27
mean γ attenuation length at 511 keV (mm)	22.4
mean γ absorption length at 511 keV (mm)	60.5

Table 1: Characteristics of YAP:Ce scintillator crystals

Introduction

Positron Emission Tomography (PET) is a non invasive, diagnostic imaging technique for measuring the metabolic activity of cells in the human body using short lived positron emitting radio-nuclides (^{18}F, ^{11}C, ^{13}N, ^{15}O, ...). The positron annihilates with an electron inside the body and produces two photons of 511 keV travelling in opposite directions that are detected in a PET scanner.

The simulation of the interaction of the photons produced in this reaction with the PET detector proposed in [1] is presented here. In addition to the detection of the gamma quanta by photoelectric effect, also a substantial fraction of Compton scattered events can be exploited. This approach allows to increase the sensitivity of the scanner by a factor 2-3.

PET Detector

The prototype of the PET detector consists of 12 inner modules and 12 outer modules located at 240 mm and 350 mm, respectively, of the interaction point, as described in [1]. The inner array is rotated by an angle $\pi/24$, with respect to the outer modules, in the XY plane (fig. 1).

Each modulus is formed by small scintillator crystals disposed in a matrix of 12×18 crystals, and it is readout on both sides by proximity focused Hybrid Photodiodes (HPD). The scintillator crystal chosen for the detection of 0.511 MeV photons has been YAP:Ce [1)] for its good physical and mechanical properties (see table 1). The dimensions of the crystals are $3.5\times3.5\times100$ mm^3 and they are equally spaced in a rectangular matrix leaving a gap of air of 0.3 mm between them (fig. 2). For the analysis presented here only the outer module located at (350,0,0) will be considered and no readout system is included.

Physics processes

The physics processes have been simulated using the low energy extension of GEANT4 where the implementation of the electromagnetic interactions is precise for energies down to 250 eV. The data used for the determination of the cross sections and sampling of the final states are extracted from the EPDL97 [2], EEDL [3] and EADL [4] libraries. The stopping power data from [5–8] and the binding energies from [9].

[1)] Cerium doped Yttrium Aluminium Perovskite

The reactions considered to simulate the photon interactions with the YAP:Ce material are:

- The Compton effect. The simulation of this process is done according to the Klein-Nishina formula [10] taking into account the Hubble's atomic form factor [11]. The angular energy distributions of the incoherently scattered photon is given by the product of the Klein-Nishina formula and the scattering function.
- The photo-electric effect. The incident photon is absorbed and an electron is emitted in the same direction as the original photon. The electron kinetic energy is the difference between the incident photon energy and the binding energy of the electron before the interaction. The sub-shells from which the electron is emitted is randomly selected according to the relativistic cross sections of all sub-shells, determined at the given energy T, by interpolating the evaluated cross section data from the EPDL97 data library. The interaction leaves the atom in an exited state. The de-excitation of the atom is also simulated as described in the GEANT4 Manual [12].
- The Rayleigh effect. The coherent scattered photon angle is sampled according to the distribution obtained from the product of the Rayleigh formula $1 + \cos^2\theta$ and the Hubble form factors squared [11].

At this step of the analysis no optical photons have been yet simulated.

Analysis of data

10000 events have been generated for the study of the interaction of the photons with the PET module. The photons are generated with an energy of 0.511 MeV along the X direction. The source where the photons are emitted is considered to be a sphere of radii 4 mm located at the centre of the PET detector and only the external module located at (350,0,0) is considered as detector.

In this configuration 25.6% of the events do not undergo any interaction in the PET module either because the photon goes through the dead zones of the detector (i.e. the gap of air between the crystals) or because the photon did not interact with any atom of the YAP:Ce material. Table 2 shows the statistics of the different processes that occurs before a photo absorption takes place or before the photon is lost undetected.

Photo-electric effect

From the events in which at least one interaction took place there are only 4.5% where a photo-electron was emitted after the first interaction. In this case the energy and position where the photon was originated can be uniquely determined ('sauf' resolutions). Figure 3 shows the absorption length for the photo-electron in the X and Y direction (each bin represents one crystal). The shape of the distribution in Y is due to the way photons are produced along the Y axis.

Figure 4 shows the path length of the photo-electron in X, Y, and Z directions. The average distance travelled by the photo-electron in the X direction is $\sim 100\mu$m, therefore in the case where the absorption takes place at the edges of the crystal the electron will get out of the crystal. In figure 5 it is represented the position where the absorption of the photon took place in one crystal, in bins of 100μm. In approximately 3% of the events the electron hits the edge of the crystal and will not be properly reconstructed.

Compton	Photo-electric	Out	Nevents
0	0	1	2089
0	1	0	358
1	0	1	1656
1	1	0	896
2	0	1	912
2	1	0	1222
3	0	1	448
3	1	0	1058
4	0	1	142
4	1	0	609
5	0	1	51
5	1	0	242
6	0	1	18
6	1	0	119

Table 2: Statistics of the different interactions. Out means that the particle escaped from the detector.

Compton Effect

Another important configuration is the case in which the photon is scattered incoherently from one of the atoms of the YAP:Ce material before a photo-electron is produced or it escapes the detector. This process can occur several times. Figure 6a shows the position where the first Compton interaction takes place for all events in which the number of Compton interactions is ≥ 1. In figure 6b the energy of the scattered photon versus the $\cos\theta$ is drawn (θ is the angle between the incident photon and the scattered one after the interaction).

After each incoherent interaction the photon looses part of its energy and changes direction. Therefore the analysis presented here will be restricted to the situation in which there is at most one Compton in the event. 20.8% of the events that have an interaction in the YAP:Ce have a Compton scattering and then escape the detector. 11.25% of the interacting events have a Compton interaction and then photo-absorption occurs (1c+1pe). These are the events we are going to study to analyse the feasibility of using them in the reconstruction of the original 0.511 MeV photon.

Figure 7a and 7b show the $\cos\theta$ distribution and the energy of the scattered photon after the Compton for 1c+1pe events. It happens often that after the Compton the photon is scattered at a large angle with respect to the incident photon (backwards scattering). When this occurs the photo-absorption will take place in a crystal located backwards. This events are called ambiguous as it is not possible to disentangle whether the Compton or the photo-absorption interactions took place first. Figure 8a displays the crystal number where the photo-absorption takes place versus the crystal number where the Compton occurs in the X direction. The crystals are numbered from 1 to 12, and all the events below the diagonal are ambiguous 1c+1pe events. In figure 8b the difference between the position of the photoelectric and the Compton, in number of crystals, is shown. All events in the negative region are the ambiguous events.

A closer study reveals that for the events that have an energy deposit after the Compton interaction and no electron is produced, there is no ambiguity in the reconstruction of the two

interaction points. Figure 9a shows that for these events the angle between the incident and scattered photon after the Compton interaction is smaller that 64°. The energy deposited by the photon is < 180 keV (fig. 9b) thus the energy of the scattered photon is larger than 330 keV (fig. 9c).

The crystal where the photoabsorption takes place is shown versus the crystal where the compton occurs in figure 10a and the difference between the position of the photelectric and Compton in number of crystals (fig. 10b). It is clear that in this cases there is no ambiguity. The photoelectric effect takes place in the same or in a crystal behind the Compton effect. This represents $\sim 2.5\%$ of the events which undergo an interaction in the detector.

The path length of the photelectron for this events is shown in figure 11 in the X, Y and Z direction. The path length of the photoelectron in the X direction is $\sim 50\mu$m. Only 1% of the events are photoabsorbed at the edge of the crystal and hence lost (fig. 12).

Conclusions

GEANT4 has been used to simulate the interaction of 511 keV photons in a modulus of a PET detector composed of 12x18 crystals of YAP:Ce material. The dimensions of the crystals used are $3.5 \times 3.5 \times 100$ mm^3 with a gap of air between them of 0.3 mm. From the 7962 events that have an interaction in the detector 358 events (i.e. 4.43%) are absorbed at the first interaction by photoabsorption and can be used to reconstruct the initial photon. From the events that undergo first a Compton interaction and then photoabsorption 202 (i.e. 2.5%) can be unambiguously reconstructed. This means that the coincidence detection probabilily is:

$$P = (0.0435)^2 + (0.02475)^2 + 2 \times 0.0435 \times 0.02475$$

$$P = 0.46\%$$

where the inefficiencies when the photoabsorption occurs at the edge of the crystal have already been takend into account.

References

[1] "A PET Detector With Parallax-free Compton Enhanced 3D Gamma Reconstruction". Private communication .

[2] "EPDL97: the evaluated Photon Data Library, 97 version". D. Cullen, J.H. Hubbell, L. Kissel, UCRL-50400, Vol. 6, Rev. 5.

[3] "Tables and Graphs of Electron-Interaction Cross sections from 10eVto 100GeVderived from the LLNL Evaluated Electron Data Library (EEDL), Z=1-100". S.T. perkins, D.E. Cullen, S.M. Seltzer, UCRL-50400, Vol. 31.

[4] "Tables and Graphs of Atomic Subshell and relaxation Data Dereived from the LLNL Evaluated Data Library (EADL), Z=1-100", S.T. perkins, D.E. Cullen, M.H.Chen, J.H. Hubbell, J. Rathkopf, J. Scofield, UCRL-50400, Vol.30 .

[5] "The Stopping and Ranges of Ions in Matter, H.H. Andersen, J.F. Ziegler Vol. 3, Pergamon Press (1977).

[6] "The Stopping and Ranges of Ions in Matter, J.F. Ziegler Vol. 4 Pergamon Press (1977).

[7] "The Stopping and Ranges of Ions in Solids, J.F. Ziegler, J.P. Biersack, U. Littmark, Vol. 1 Pergamon Press (1985).

[8] "Stopping Powers and Ranges for Protons and Alpha Particles", A. Allisy *et al.* ICRU Report 49, (1993).

[9] "Radiative Transitions in Atomic Inner-Shell Processes" J.H. Scofield, B. Crasemann ed., Academic Press New York (1975) 265.

[10] D.E. Cullen "A Simple Model of Photon Transport", Nucl. Ins. Meth. Phys. Res. **B 101** (1995) 499.

[11] "Summary of Existing Information on the Incoherent Scattering of Photons particularly on the Validity if the Use of the Incoherent Scattering Functions", Radiat. Phys. Chem. Vol 50, No 1 (1997) 113.

[12] GEANT version 4.4.0 is used; .

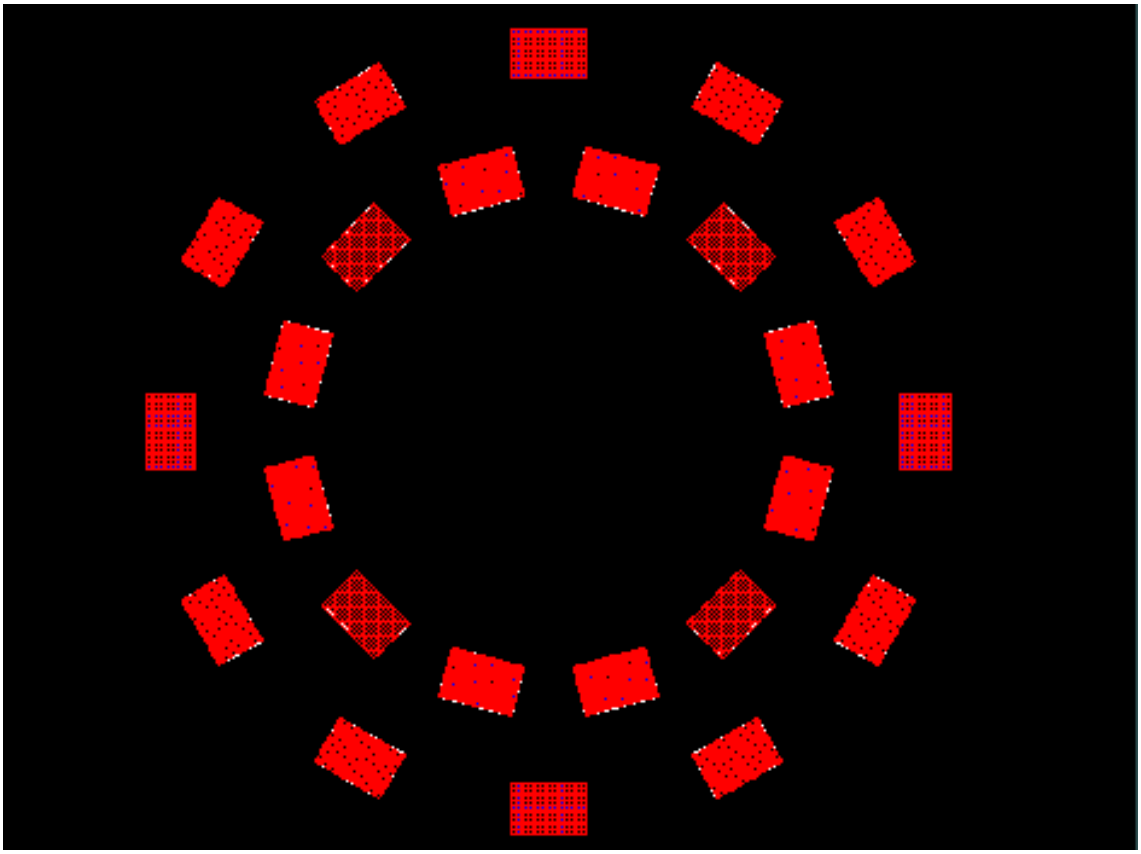

Figure 1: View of the inner and outer modules of the PET detector in the XY plane.

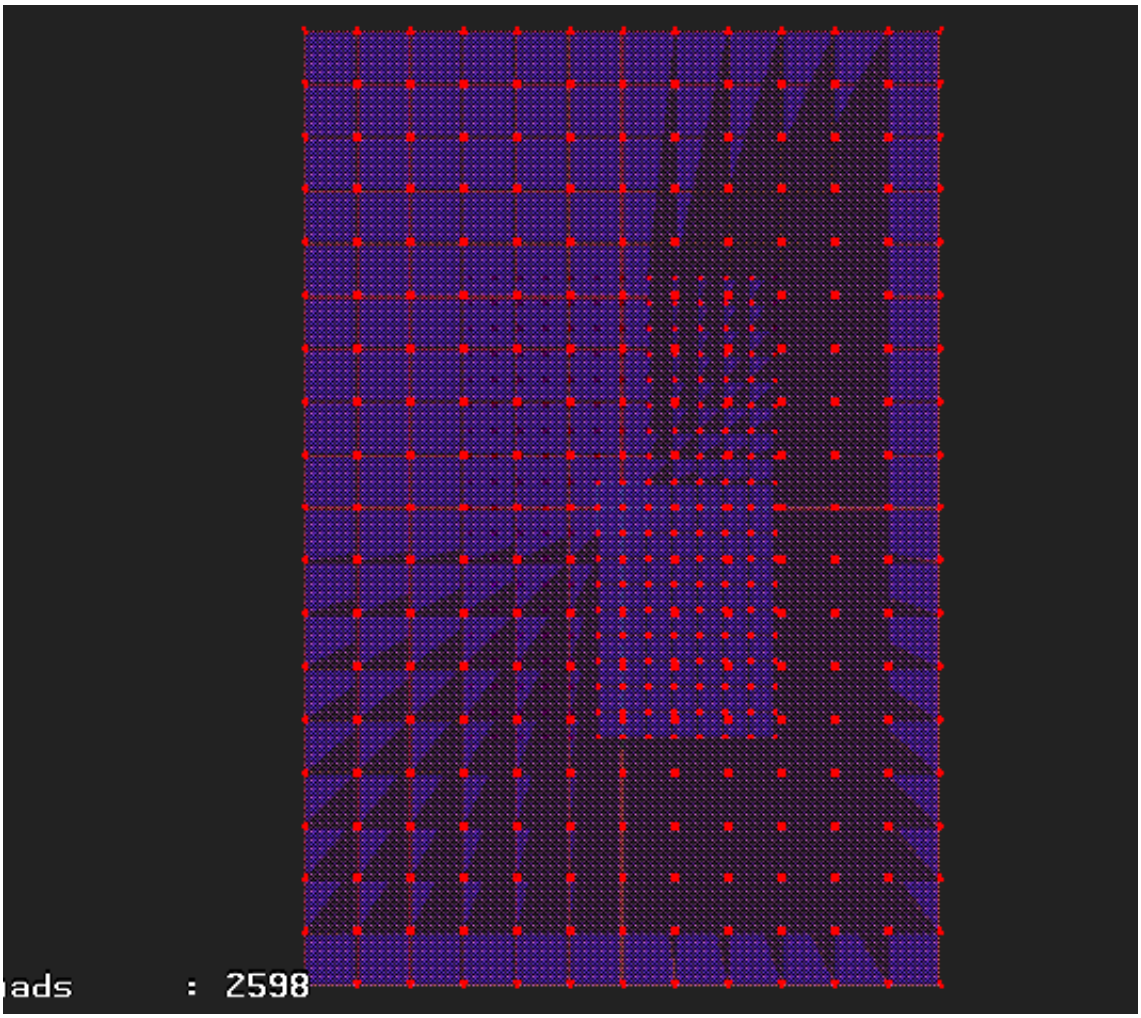

Figure 2: XY view of one PET module without the readout system. In the figure it is only shown the 12×18 matrix of scintillator cystals.

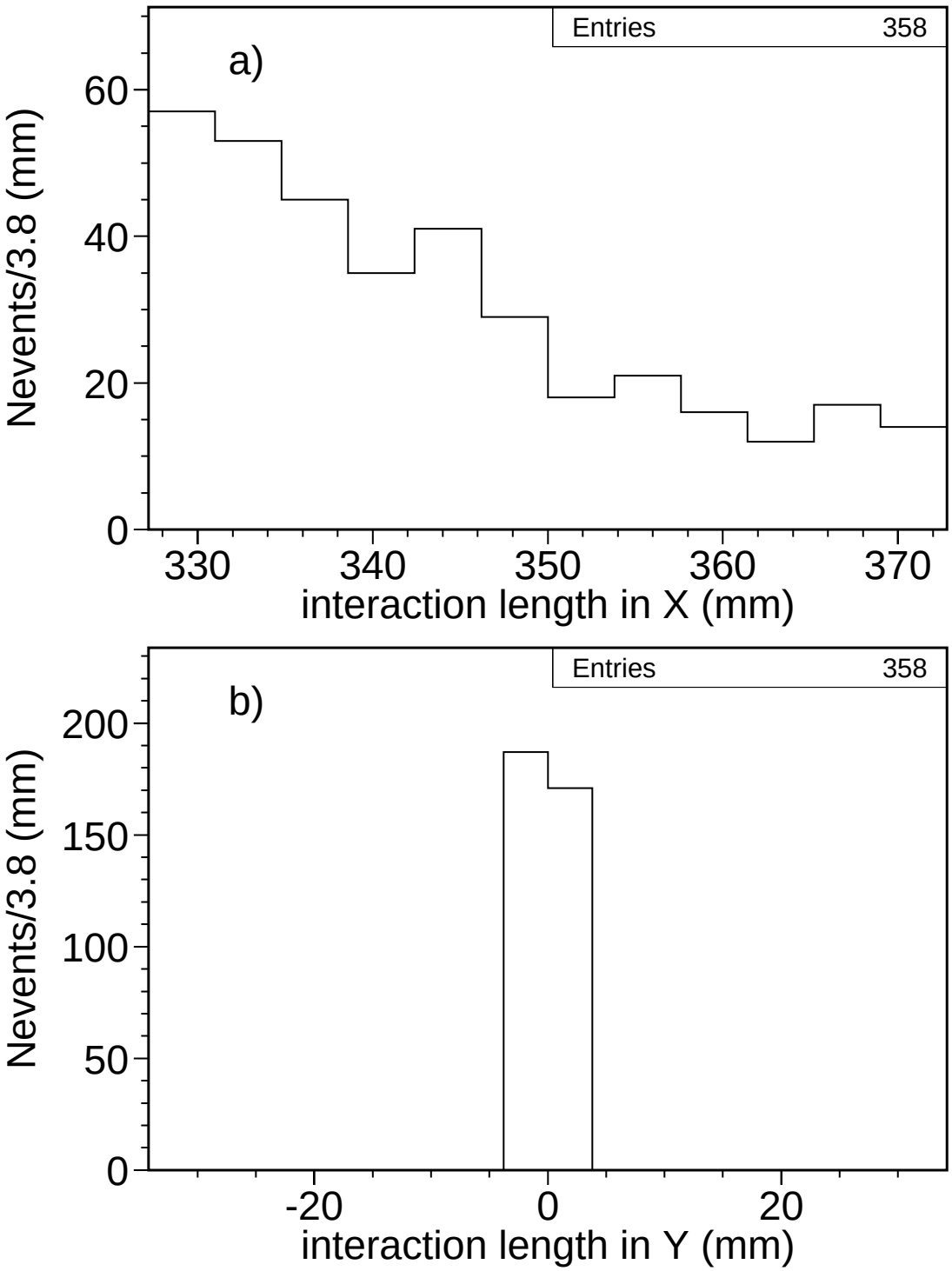

Figure 3: Position in X (up) and Y (down) where the photoelectric effect takes place for events with no other interaction.

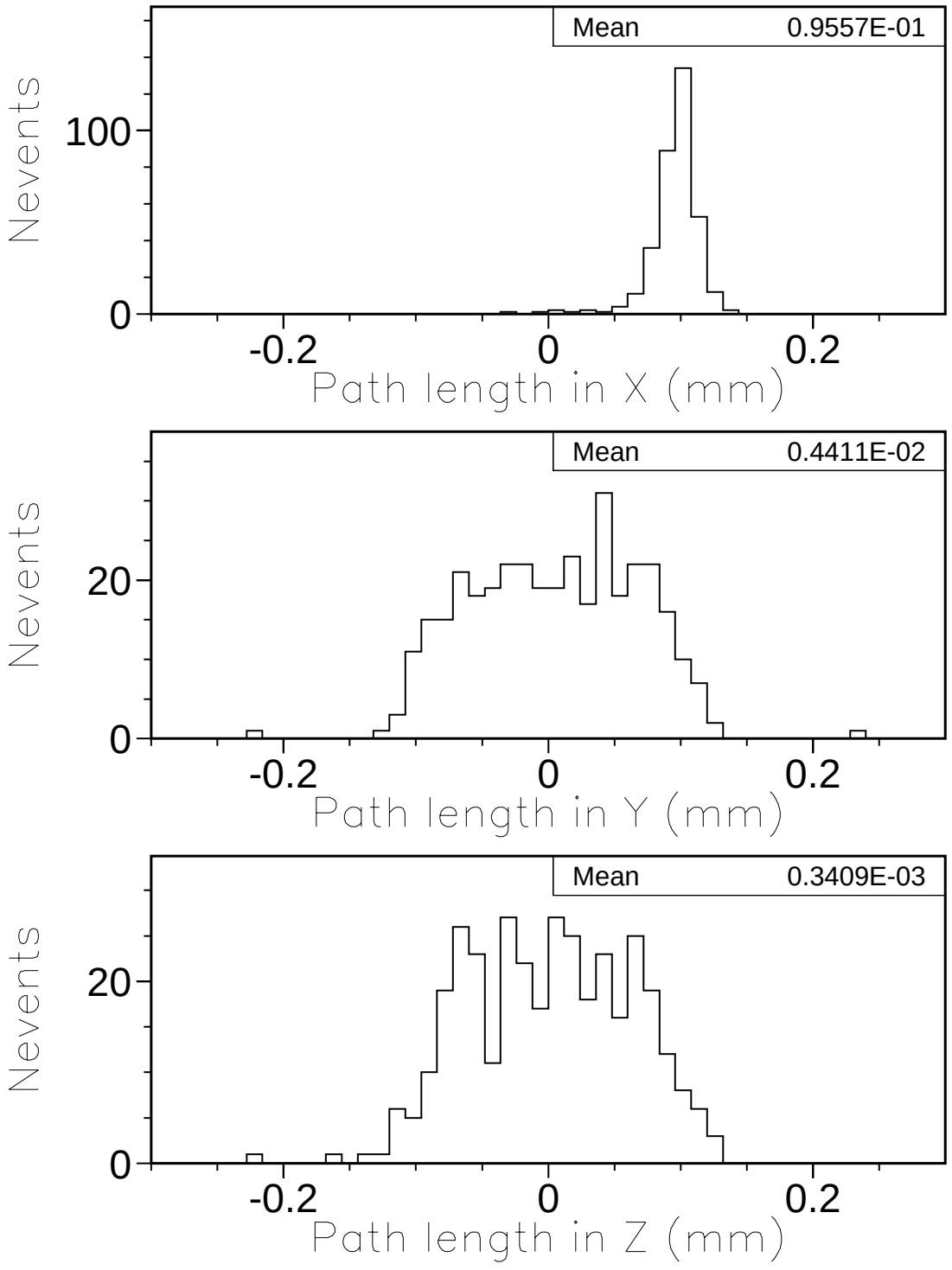

Figure 4: Path lenght in X, Y and Z of the photo-electron.

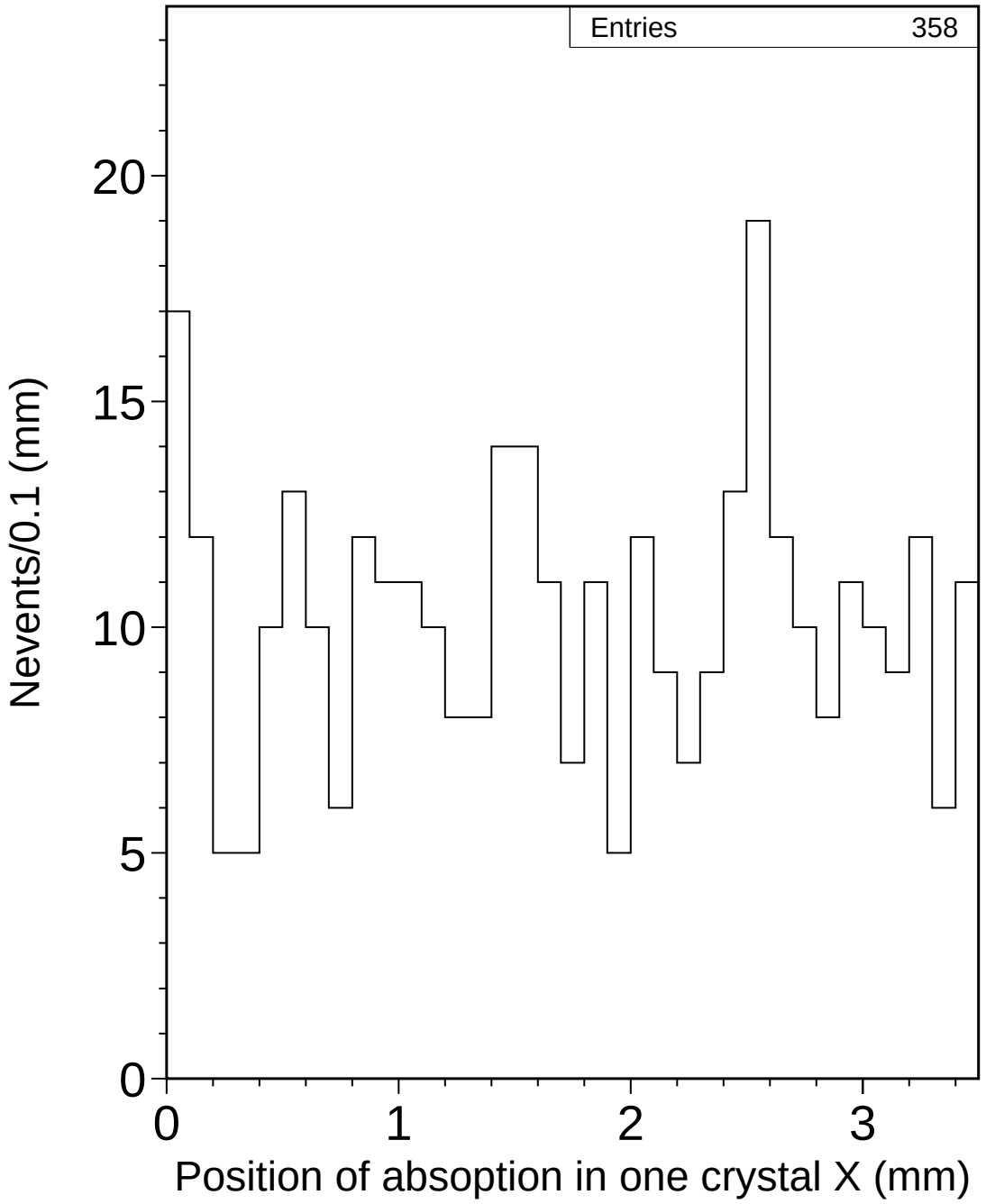

Figure 5: Position in X (up) and Y (down) where the photoelectric effect takes place in the crystal.

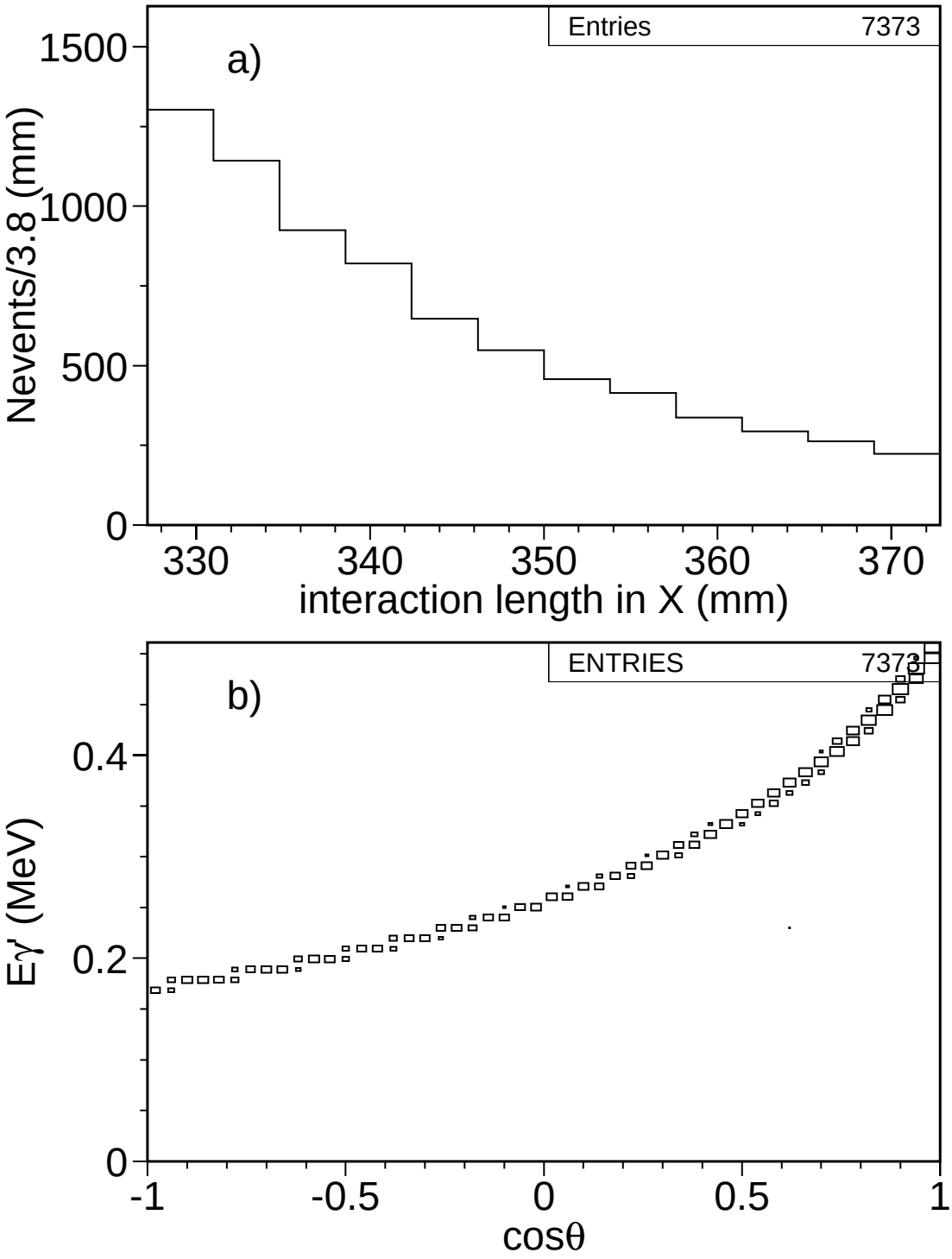

Figure 6: a) Position in X where the first Compton interaction takes place. b) Energy of the scattered photon versus cosθ, where θ is the angle between the incident photon and the scattered one after the first scattering. In both figures all events with at least a Compton interaction are considered.

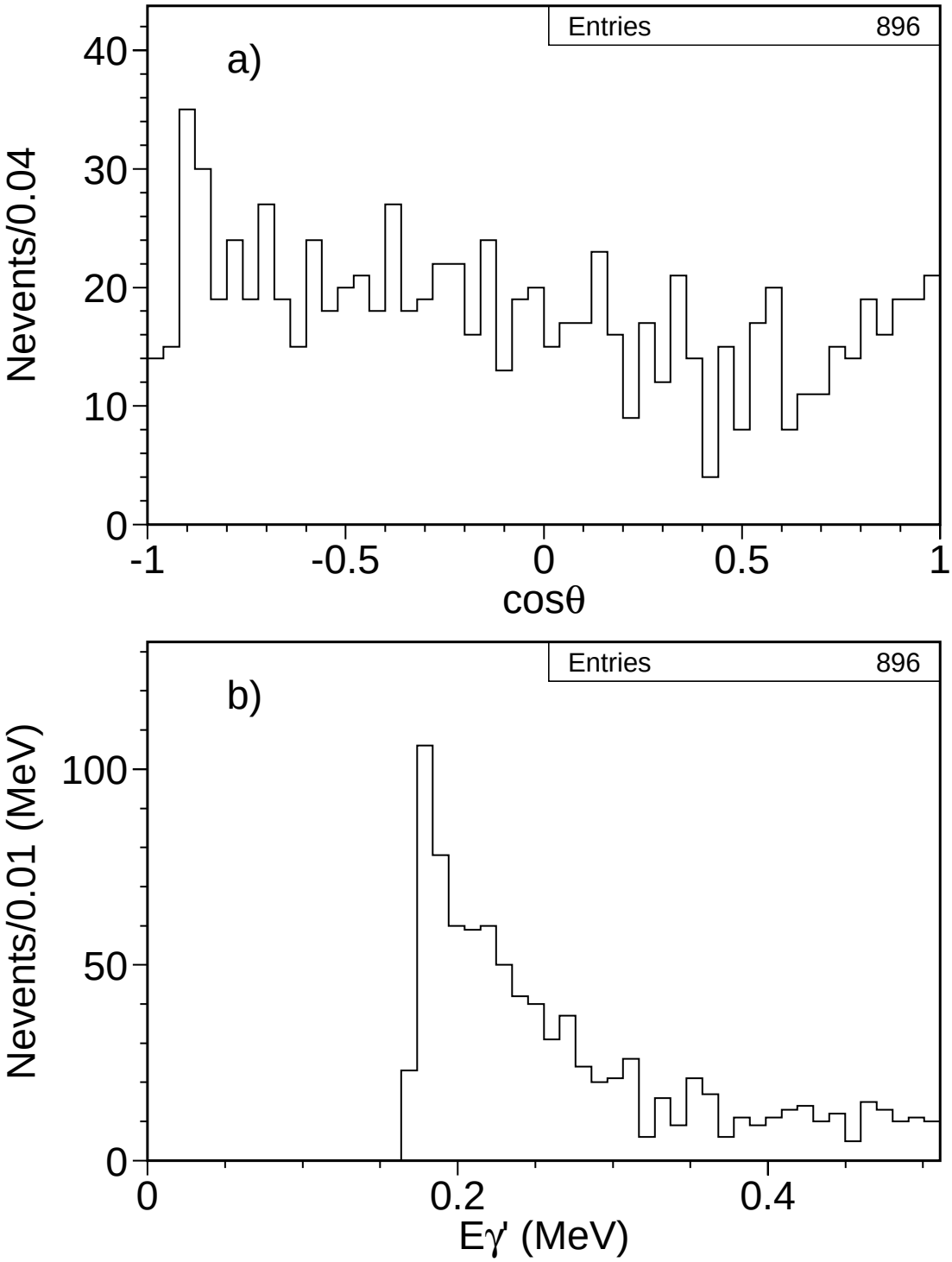

Figure 7: a) $\cos\theta$ distribition after the Compton interaction for events in which there is a Compton and then a photoabsoption. b) Energy of the scattered photon after the Compton for the same envents.

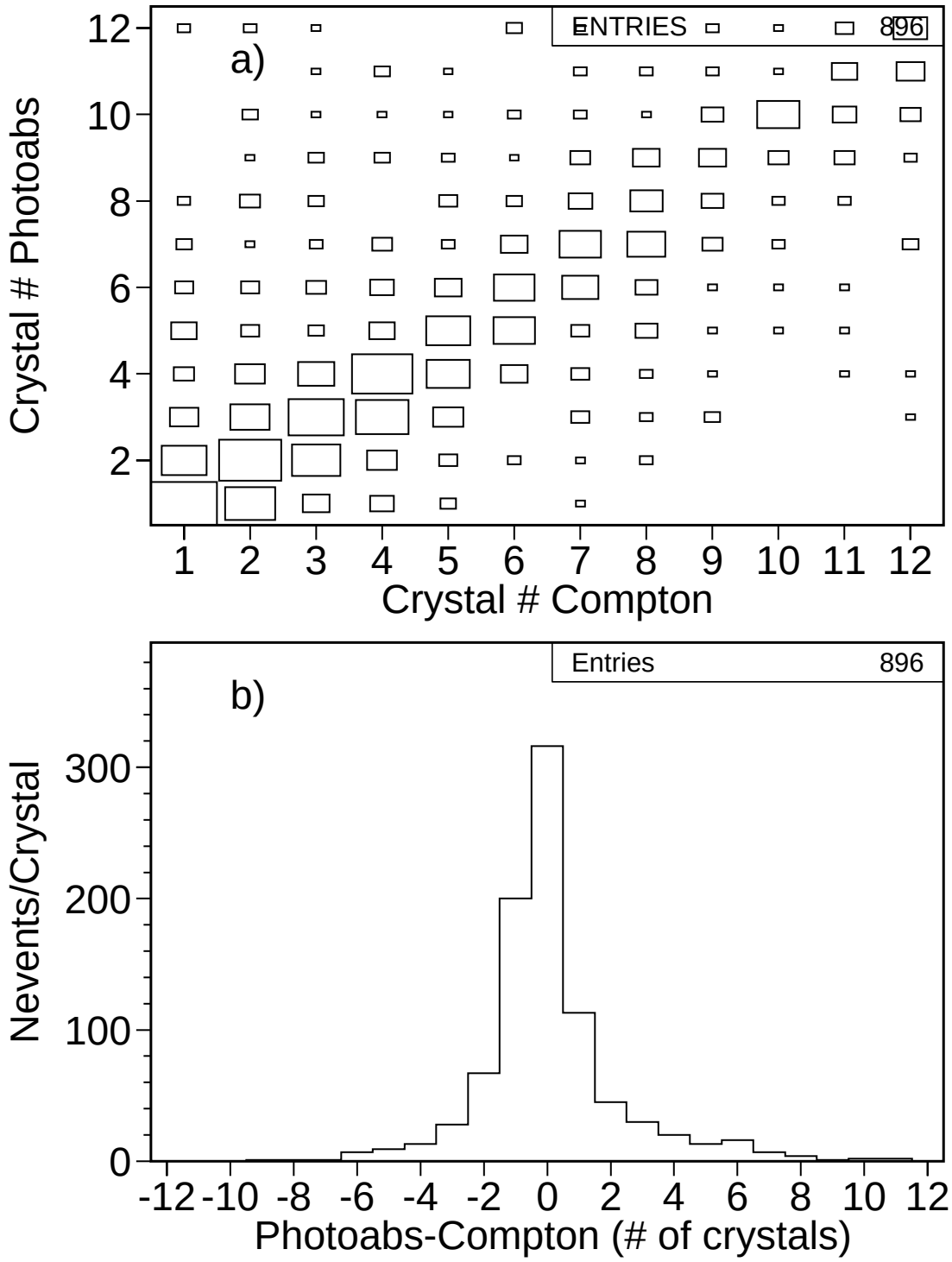

Figure 8: a) Number of crystal where the photoabsorption takes place versus the number of crystal where the Compton occurs in X for 1c+1pe events. b) Difference in number of crystals between the position of the photoabsoption and the Compton in X.

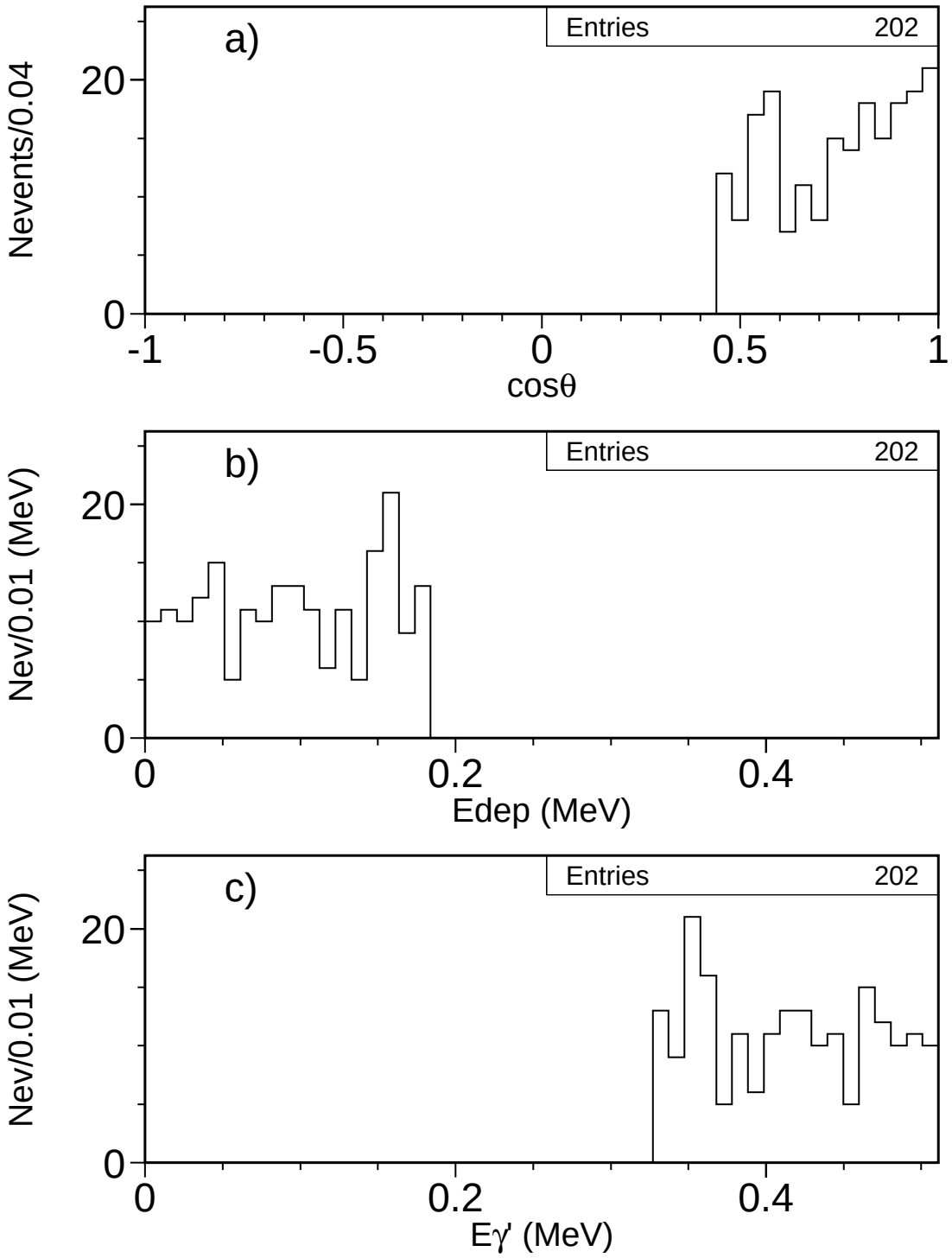

Figure 9: a) $\cos\theta$ of the scattered photon and the incident photon for 1c+1pe events when there is no electron track. b) Energy deposit after the compton interaction. c) Energy of the scattered photon after the Compton.

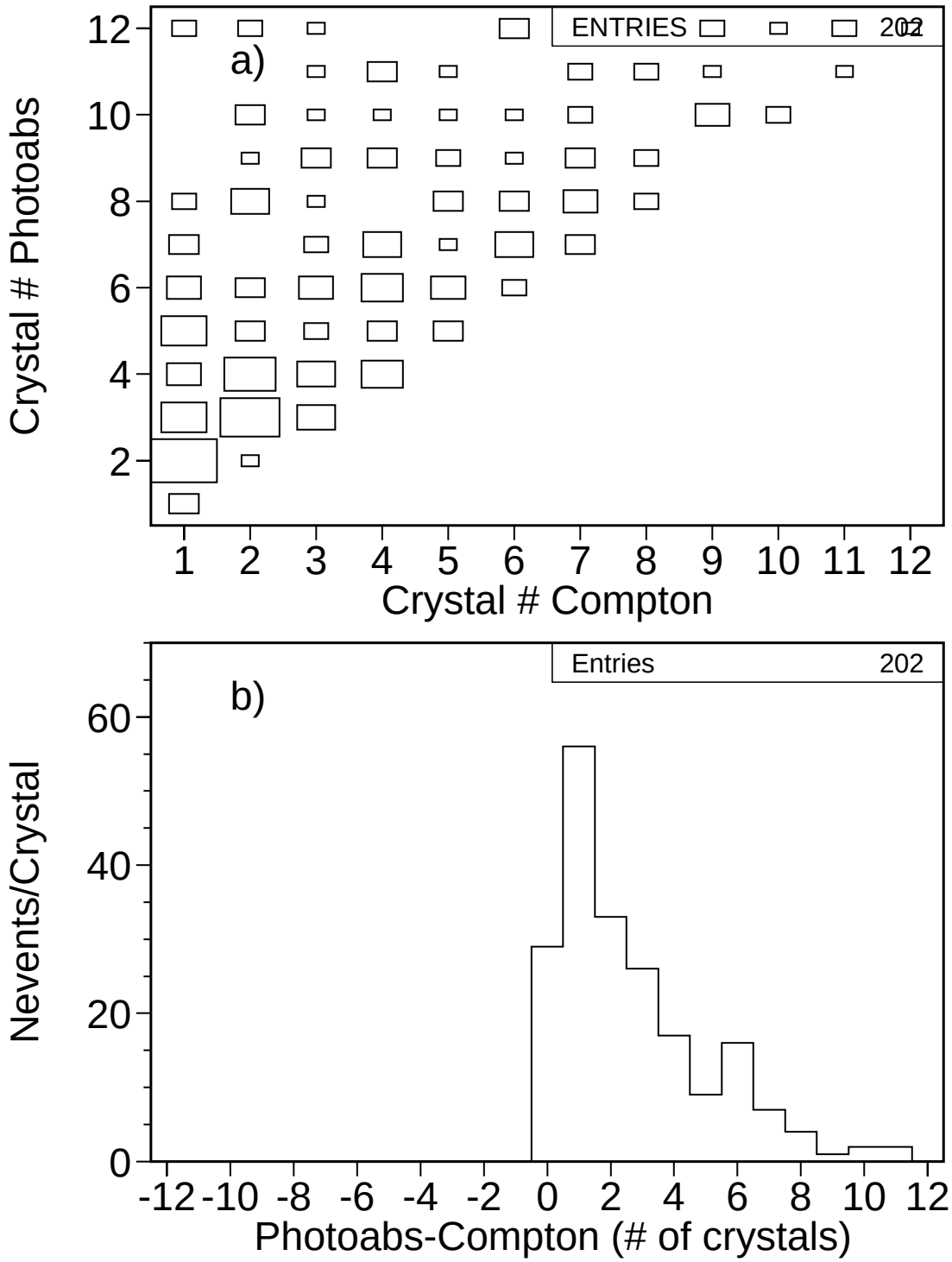

Figure 10: a) $\cos\theta$ of the scattered photon and the incident photon for 1c+1pe events when there is no electron track. b) Energy deposit after the compton interaction. c) Energy of the scattered photon after the Compton.

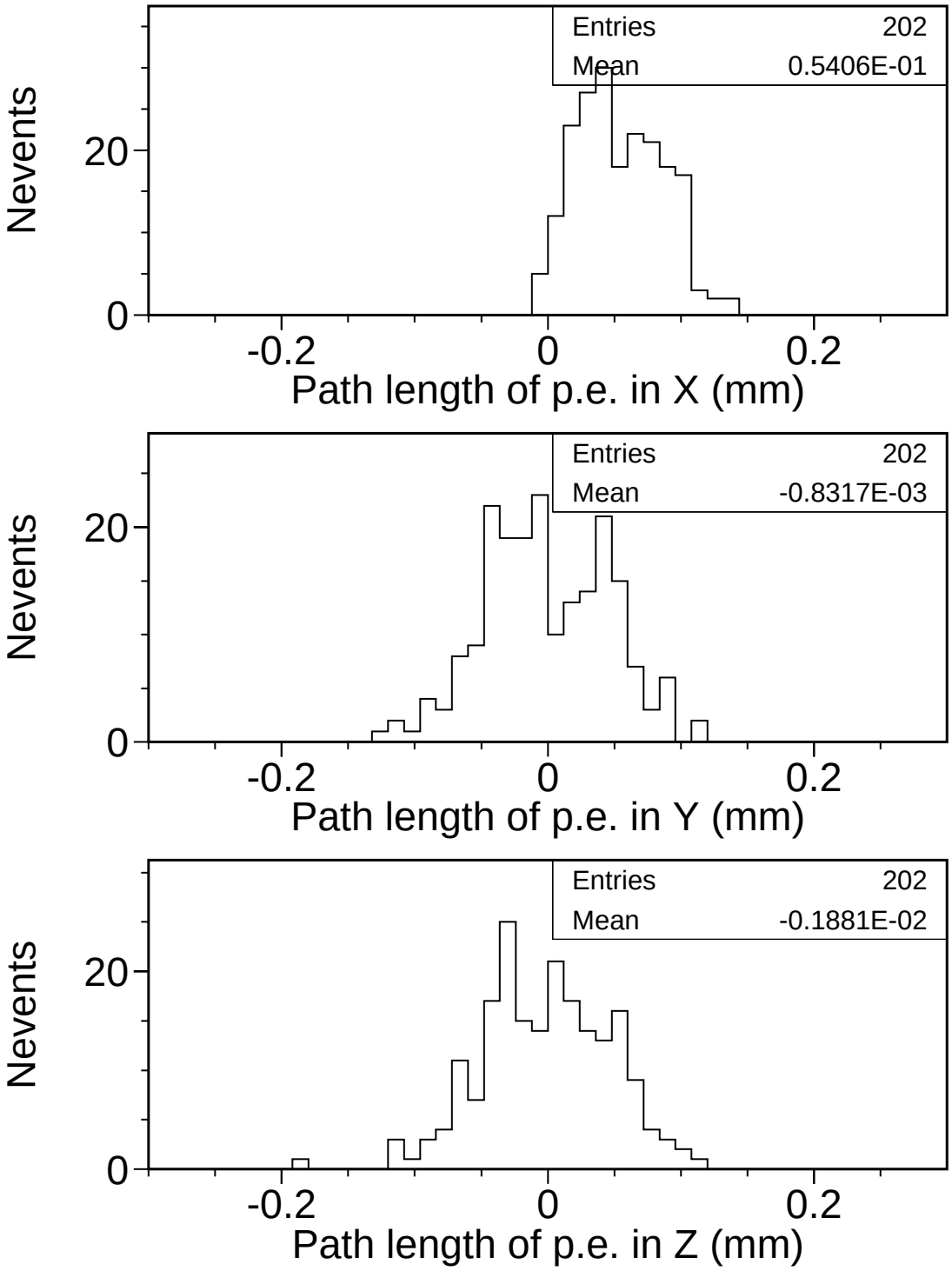

Figure 11: Path lenght of the photoelectron for 1c+1pe events with an energy deposit after the Compton in a) X direction b) Y direction c) Z direction.

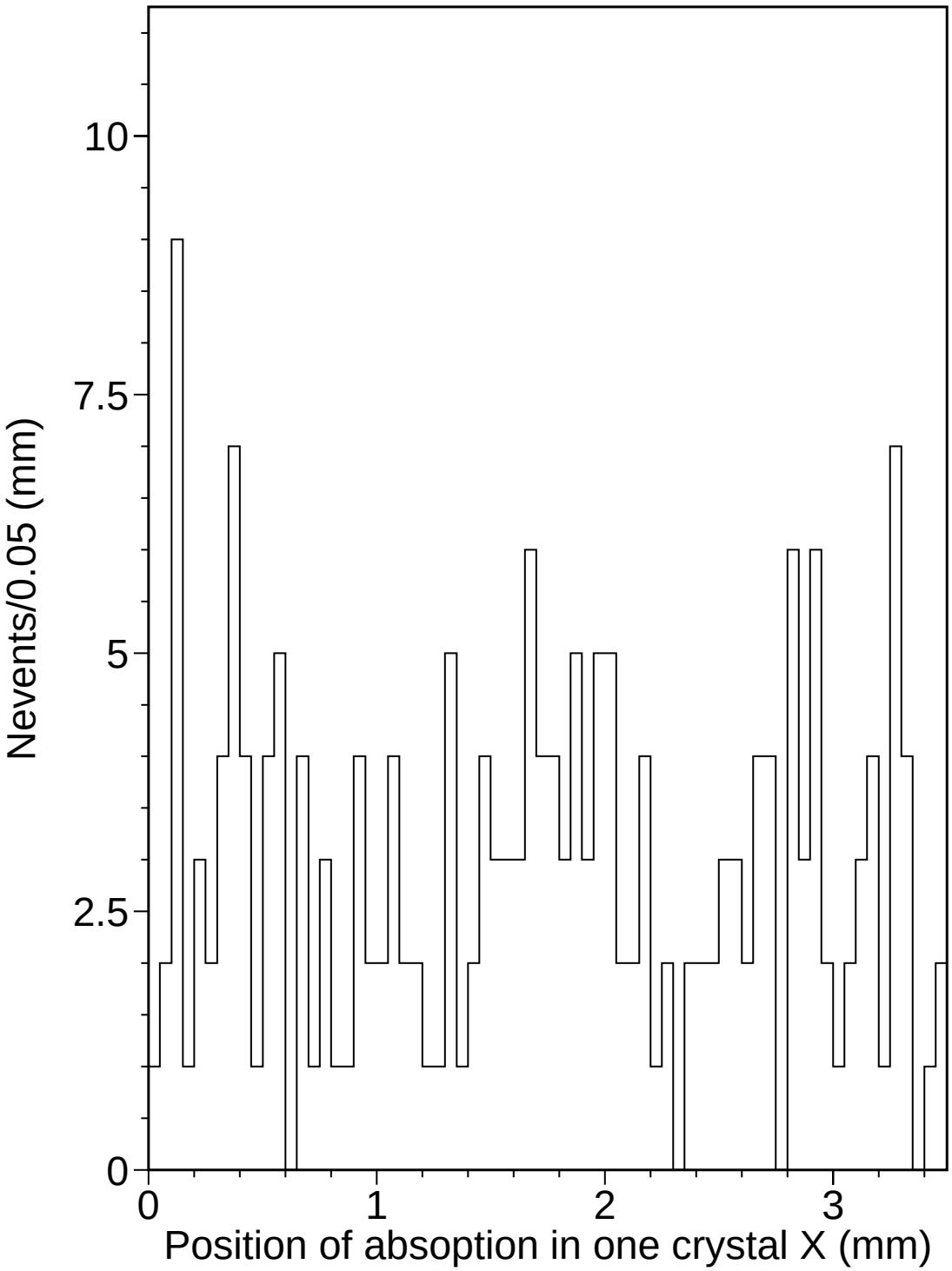

Figure 12: Path lenght of the photoelectron for 1c+1pe events with an energy deposit after the Compton modulo one crystal.